

Donepezil-Squaric Acid Hybrid: Synthesis, Characterization and Investigation of Anticholinesterase Inhibitory, DNA Binding and Antioxidant Properties

Derya Kılıçaslan^{1,2,a,*}¹ Afsin Vocational School, Department of Chemistry and Chemical Processing Technologies, Kahramanmaraş Sutcu Imam University, Kahramanmaraş, Türkiye² Research and Development Centre for University-Industry-Public Relations, Kahramanmaraş Sutcu Imam University, Kahramanmaraş, 46050, Türkiye

*Corresponding author

Research Article

History

Received: 03/01/2024

Accepted: 14/06/2024



This article is licensed under a Creative Commons Attribution-NonCommercial 4.0 International License (CC BY-NC 4.0)

ABSTRACT

A novel donepezil-squaric acid (DS) hybrid compound was designed, synthesized and biologically evaluated as multi-target-directed ligands against neurodegenerative disease by fusing a fragment of donepezil (D) and squaric acid (S). This study focuses on investigating the binding mechanism of double-stranded fish sperm DNA (Fsds-DNA) with DS and S. The interaction between DS and S with Fsds-DNA was explored using spectrophotometric and viscometric methods. Besides, DNA binding constants (K_b) were determined. The results reveal that DS binds to Fsds-DNA via the minor groove binding mode. The hybrid molecule demonstrates potent inhibitory activity against acetylcholinesterase (AChE) and butyrylcholinesterase (BuChE). Furthermore, it exhibits significant antioxidant activity, surpassing the scavenging ability of 2,2-diphenyl-1-picrylhydrazyl (DPPH) radicals compared to squaric acid alone. In conclusion, these results suggest that the hybrid molecule may serve as a potential multifunctional agent for the treatment of Alzheimer's disease.

Keywords: Donepezil, Squaric acid, DNA binding, Acetylcholinesterase, Butyrylcholinesterase.^a deryatnc@ksu.edu.tr <https://orcid.org/0000-0001-7830-8214>

Introduction

Alzheimer's disease (AD) is an irreversible neurological disorder that leads to cognitive impairment, the loss of cholinergic neurons at basal forebrain synapses and neuronal death. The etiology of AD is intricate and definitive therapeutics are still unavailable. A variety of pathological features contributes to the pathogenesis of AD, encompassing low acetylcholine level, increased monoaminoxidase concentration, oxidative stress, A β accumulation, inflammation, intracellular neurofibrillary tangles, metal ion dysregulation, etc [1]. The precise pathology of AD remains unknown in spite of ongoing research [2]. For a considerable period, researchers have concentrated on boosting acetylcholine (ACh) levels in patients' brains through inhibiting the enzyme acetylcholinesterase (AChE). Acetylcholinesterase inhibitors (AChEIs) stand out as the most commonly prescribed treatment strategy for AD. AChEIs have exhibited the ability to diminish disease progression and enhance attention span. These compounds demonstrate unique patterns of structural diversity, each having distinctive features tailored for various types of ChE. Following the introduction of AChEIs, cholinergic drugs such as galantamine, donepezil and rivastigmine emerged as primary pharmacotherapy options for mild to moderate AD [3]. Nevertheless, controlling the progression of AD necessitates more than inhibiting a single underlying cause; instead, it requires simultaneous modulations of all relevant types. This comprehensive approach is achieved through studies focused on

designing and synthesizing multi-targeted ligands for AD therapy [4].

Squaric acid serves as a functional structural scaffold that can be readily transformed into amide-containing compounds featuring both hydrogen bond donor and acceptor groups. This characteristic offers the potential for forming multiple interactions with complementary sites [5]. The squaric acid scaffold is a unique molecule that has garnered significant interest, particularly in the last decade, owing to its diverse applications in synthetic [6], pharmaceutical [7] and other fields [8-12]. Squaric acid, (also known as quadratic acid; 3,4-dihydroxycyclobut-3-en-1,2-dione), adopts a planar aromatic framework and derives its distinctive name from its square shape. Its analogues exhibit various biological activities, activated by the presence of crucial H-bond donors and acceptors [13]. Squaric acid analogues hold significance in medicinal chemistry for several reasons. Firstly, unlike many other compounds designed as potential drugs, they typically do not exhibit high lipophilicity and low solubility in water. The resultant compounds demonstrate enhanced solubility, rendering them suitable as therapeutic agents particularly when squaric acid or the squaramide scaffold is combined with amine and carboxylic groups [14,15]. Besides, analogues of carboxylic acid may function as non-classical isosteres for carboxylates and amino acids in the course of drug

development [16]. The utilization of chlorogenic acid analogues in chemical biology is predominantly exemplified by their bioconjugation to proteins or carbohydrates and their application as ion receptors. Conversely, in medicinal chemistry, these compounds possess diverse biological effects, involving antichagasic, antiplasmodial, anticancer and antibacterial activity, positioning them as promising agents in drug development. Squaramide can be regarded as a noteworthy motif that facilitates the formation of H-bonds bioisosteric to functionalities like carboxylic and amino acids, guanidine urea, cyanoguanidine and various phosphate groups [16]. Squaric acid occupies a unique position among oxocarbonic acids as it has an equal number of atoms that act as donors and acceptors for the formation of hydrogen bonds. This ligand can behave quite differently depending on the conditions because it has a highly symmetrical ring structure and tends to form chains with hydrogen bonds. It also has a structure suitable for forming two- or three-dimensional structures. The equal number of acceptor and donor oxygen atoms and the planar ion form with squaric acid allow the synthesis of polymeric, two- and three-dimensional supramolecular structures. There are mixed ligand complexes containing squaric acid in the literature [17-19]. A commercial AChE inhibitor, donepezil is employed in the treatment of mild to moderate AD. In addition, it has garnered widespread attention due to its potent AChE inhibitory properties, low toxicity, high selectivity and favorable bioavailability [20]. The 1-benzylpiperidine fragment within donepezil serves as the crucial pharmacophore of AChE inhibition, contributing to its good solubility in water, and numerous donepezil hybrids have been developed as multi-target-directed ligands [21-23]. Considering the relatively simple synthesis approach of the squaramide motif and its appealing properties (rigidity, aromatic character, H-bond formation), we opted to combine this scaffold with donepezil. This study endeavours to create a multi-target active small molecule by merging squaric acid with donepezil, aiming to assess whether the new molecule exhibits diverse multifunctional potential and good drug-like properties. We synthesized a novel squaric acid-donepezil hybrid and developed it as a multi-target-oriented ligand in the current study. It also focused on the binding mechanism of Fds-DNA with DS and S. UV-vis absorption spectroscopy, fluorescence spectroscopy and viscosimetry were deployed to explore the interaction between the molecules and Fds-DNA. Furthermore, the interaction of Fds-DNA and DS was compared with the S interaction. The evaluation encompassed AChE and BuChE inhibitory activity as well as antioxidant activity.

Experimental

Apparatus

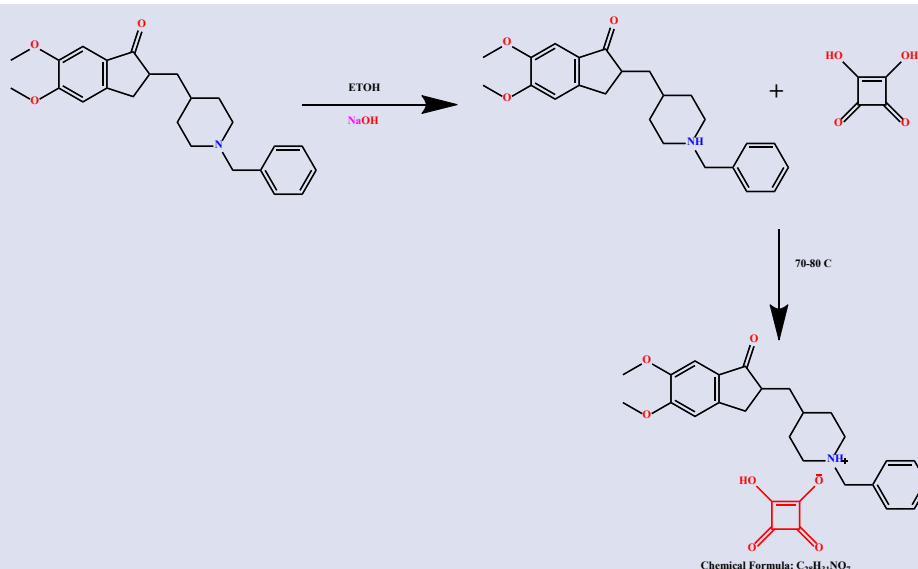
For the analysis of the IR spectra of the DS and S, we employed the Attenuated Total Reflectance technique and conducted measurements on the Perkin Elmer Spectrum 100 FT-IR Spectrophotometer. The results were assessed in wavenumbers (cm^{-1}). ^{13}C NMR and ^1H spectra were acquired using the Bruker AVANCE III 400 MHz NMR Spectrometer with DMSO- d_6 as the solvent. Chemical shift values (ppm) were determined on the δ scale with the solvent serving as the reference peak, and interaction constants were presented in Hertz (Hz). AChE and BuChE enzyme inhibition activities, along with antioxidant activity, were determined using the Hitachi U3900H Spectrophotometer. UV-vis absorption studies were conducted using a Perkin-Elmer Lambda 25 spectrometer. Compound photoluminescence spectra were measured with a Perkin Elmer LS55 spectrometer.

Chemicals

Starting materials donepezil hydrochloride reagent-grade analytical standard $\geq 98\%$ (HPLC) was procured from ARIS (Ali Raif Ilaç Sanayi, Istanbul, Turkey) and used as received. Squaric acid (3,4-Dihydroxy-3-cyclobutene-1,2-dione) and solvents were purchased from commercial sources (Sigma-Aldrich, Germany) and used as received. Electric eel AChE (Type-VI-S, EC 3.1.1.7, Sigma) and horse serum BChE (EC 3.1.1.8, Sigma) were used, while acetylthiocholine iodide and butyrylthiocholine chloride (Sigma, St. Louis, MO, USA) were employed as substrates of the reaction. 5,5'-Dithio-bis(2-nitrobenzoic)acid (DTNB, Sigma, St. Louis, MO, USA) was used for the measurement of the anticholinesterase activity. In addition, 2,2-Diphenyl-1-picrylhydrazyl (DPPH) was obtained from Sigma-Aldrich- Germany.

Procedure

The synthesis procedure consists of two steps. In the first part, Donepezil hydrochloride was dissolved in 0.24 mmol (0.1 g) ethanol. Then, 0.24 mmol (0.0096 g) NaOH was added and the mixture was stirred under reflux for 2 hours. The resulting NaCl was filtered off and the reaction mixture was stirred for another 2 hours. In the second part, 0.24 mmol (0.0273 g) of squaric acid (5/2 ml DMF/ H_2O) was added. The reaction mixture was kept under reflux at 70-80 °C for 6 hours. Slow evaporation of the solvent gave a powdery cream-colored product. The product was filtered and washed with water (Scheme 1). The progress of the reaction was monitored by TLC. The purity of the product was evaluated by single spot TLC under UV lamp.



Scheme 1. Synthesis of DS

DS: $C_{28}H_{31}NO_7$, MW: 493.56 g/mol, Yield: %92 Color: cream, FT-IR (ATR cm^{-1}): 3357 (O-H), 2929 (C-H), 2702 (N-H) 1797 (C=O), 1665 (C=C). 1H NMR (DMSO- d_6 , ppm): 4.07 ($CH_{2phenyl}$), 5.05 (NH) 7.05-7.50 ($CH_{aromatic}$), 1.26-2.67 ($CH_{aliphatic}$), 3.79 (OCH_3), 3.87 (OCH_3). ^{13}C NMR (DMSO- d_6 , ppm) δ 206.7 (C=O indole), 155.79-104.31 ($C_{aromatic}$), 56.39 and 55.89 (OCH_3), 59.65 (C_{phenyl}), 51.71-28.28 ($C_{aliphatic}$). 197.16-196.76 (C_{squat} anion) HRMS (ESI) (m/z) [M+H]⁺: Anal. calcd. for $C_{28}H_{31}NO_7$: 493.21, Found: 495.24.

Interaction Studies of Compounds with DNA DNA Binding Studies

The DNA sample employed for assessing the compounds' binding affinity was directly sourced as double-stranded fish sperm DNA (Fsds-DNA) procured from Aldrich without any specific purification. Tris-HCl buffer was formulated using 20 mM Tris-HCl and 20 mM NaCl in pH 7 medium. A fresh stock solution of Fsds-DNA (5 mg ml^{-1}) was prepared, and the concentration of the resulting Fsds-DNA solution was determined by measuring the absorbance at 260 nm. A known value of the molar extinction coefficient of $6600\text{ M}^{-1}\text{ cm}^{-1}$ was used to calculate the concentration.

Stock solutions of compounds ($1 \times 10^{-3}\text{ M}$) were prepared in DMSO as co-solvent and buffer as solvent. The assay was carried out in the presence of a constant concentration of DS and S ($2 \times 10^{-4}\text{ M}$) and by titrating the increasing concentration of Fsds-DNA. The Fsds-DNA concentration per nucleotide was determined through absorption spectroscopy, utilizing the molar absorption coefficient ($6600\text{ M}^{-1}\text{ cm}^{-1}$) at 260 nm [24]. The binding constants (K_b) of the DS and S were calculated by plotting $[DNA]/(\epsilon_a/\epsilon_f)$ versus $[DNA]/(\epsilon_a/\epsilon_f)$, taking into account the degradation of the absorption bands of the DS and S. The following equation was used for the calculation;

$$[DNA]/(\epsilon_a - \epsilon_f) = [DNA]/(\epsilon_b - \epsilon_f) + 1/K_b(\epsilon_b - \epsilon_f)$$

[DNA] is the concentration of Fsds-DNA in base pairs, ϵ_a is the extinction coefficient ($A_{obs}/[compound]$), and ϵ_b and ϵ_f are the extinction coefficients of the free and fully bound forms, respectively. In $[DNA]/(\epsilon_a/\epsilon_f)$ vs $[DNA]$ plots, K_b is depicted by the intersection ratio of the slope [24].

Fluorescence Competitive Binding Studies

Competitive ethidium bromide (EB) binding studies were conducted to assess the relative binding affinities of S and DS to Fsds-DNA, employing the fluorescence spectroscopy technique. Fluorescence intensities of ethidium bromide bound to Fsds-DNA were measured at 610 nm upon excitation at 526 nm. The measurements were performed in the presence and absence of compounds (0-100 μM) in Tris-HCl buffer (2 mM Tris-HCl, pH 7.1). The Quenching constant (K_{sv}) value was calculated using the Stern-Volmer equation, derived from the graph generated using the collected data [24].

$$F_0/F = K_{sv} [Q] + 1,$$

Where F_0 represents the fluorescence intensity in the absence of the quencher; F represents the fluorescence intensity in the presence of the quencher; K_{sv} denotes the quenching constant, and $[Q]$ signifies the quencher concentration. The K_{sv} value was determined by plotting the F value against $[Q]$ and obtaining the slope.

Viscosity Measurement

A viscosity experiment was conducted on Ostwald's viscometer immersed in a thermostated water bath maintained at $25 \pm 1\text{ }^\circ\text{C}$. The flow times of the Fsds-DNA solution, in the presence of increasing concentrations of DS and S, were recorded with an accuracy of $\pm 0.01\text{ s}$ using a digital stopwatch. Each sample was measured three times at room temperature. The Fsds-DNA concentration was kept constant (200 μM) and the concentration of S and DS compounds varied from 0 to 60 μM . The relative

viscosity for FSds-DNA in the absence (η_0) and presence (η) of the S and DS was calculated using the formula; $\eta = (t - t_0) / t_0$ (where 't' is the flow time for the buffer solution containing FSds-DNA and the compounds at a specific concentration and 't₀' is the observed flow time for the buffer solution alone) and $\eta_0 = (t - t_0) / t_0$ (where 't' is the observed flow time for buffer solution containing FSds-DNA and 't₀' is the observed flow time for buffer solution alone). The relative viscosity (η / η_0)^{1/3} versus 1/R was then plotted, where R = concentration of DNA/concentration of DS or S [25].

Evaluation of Cholinesterase Inhibitory Activity

The AChE and BuChE inhibitory activities of the S and DS were identified through the modified Ellman method using AChE and BuChE. The inhibitory activities of the target compound were compared with those of S. All assays were conducted in a pH 8.0, 0.1 M KH₂PO₄/K₂HPO₄ buffer. The enzyme solutions were prepared at a concentration of 0.22 units/mL. A modified Ellman's method was employed using a 96-well plate reader for the in vitro measurement of AChE activity [26]. Each well consisted of 100 μ L of potassium phosphate buffer (KH₂PO₄/K₂HPO₄, 0.1 M, pH 8), 20 μ L of the sample dissolved in 50% methanol and 50% DMSO and 20 μ L of the enzyme. The mixture was pre-incubated for 15 minutes at room temperature. The chromatographic reagent 5,5-dithio-bis(2-nitrobenzoic acid) (DTNB) (3 mM, 50 μ L/well) and substrates acetylthiocholine iodine (ATCI) (3 mM, 50 μ L/well) or butyrylthiocholine iodine (BTCl) (3 mM, 50 μ L/well) was added to the enzyme-inhibitor mixture. The yellow anion (2-Nitro-5-thiobenzoic acid) formation was monitored at 412 nm for a duration of 10 minutes. An identical solution was prepared by including the enzyme without the tested compounds (as a control). Control and inhibitor readings were corrected with a blank read. Each concentration was assayed in triplicate. The concentrations of samples that inhibited the degradation of substrates (acetylcholine or butyrylcholine) by 50% (IC₅₀) were determined through linear regression analysis between percent inhibition and sample concentration using an Excel program.

Antioxidant Activity Assay

The method involves measuring the scavenging effects of antioxidants on DPPH (1,1-diphenyl-2-picrylhydrazyl) radical, a stable organic nitrogen radical. 9.86 mg DPPH was weighed and dissolved in methanol to achieve a total volume of 25 mL, resulting in the preparation of a DPPH solution. Varying concentrations of S and DS (1750 to 54 μ M) were then added to 100 mM concentration of the DPPH solution. The quenching of the absorbance at 517 nm of the DPPH radical was monitored at regular time intervals (0-45 min). All experiments were conducted in triplicate, and the mean absorbance was measured to calculate the percentage of inhibition using the following equation.

$$\% \text{ Inhibition of the DPPH free radical} = [(A_{\text{blank}} - A_{\text{sample}}) / A_{\text{blank}}] \times 100\%$$

In which A_{blank} represents the absorbance of the DPPH radical in the absence of a sample, and A_{sample} is the absorbance of the DPPH radical in the presence of varying concentrations of sample [27,28]. The radical inhibition concentration (IC₅₀) of S and DS was determined from the plot of the percentage inhibition versus the sample concentration.

Results and Discussion

Two donor O-H groups and two carbonyl acceptors are present in squaric acid, while there is one donor and three proton acceptors in the monoanion structure. The IR spectrum of the synthesised DS complex was analyzed and the characteristic vibrations were identified. The relationship between the structures D and S forming DS and their spectra was investigated. The IR spectrum of squaric acid was initially examined to explore the similarities and differences between the IR spectrum of DS and the IR spectrum of squaric acid. Four characteristic and strong peaks were observed in the 4000-200 cm⁻¹ range in both the IR spectrum of squaric acid and DS. A strong broad peak around 1505 cm⁻¹ was evident, representing a mixture of C-C and C-O stretching vibrations. The peak at 1652 cm⁻¹ is associated with $\nu(\text{C}=\text{C})$ stretching vibrations. The $\nu(\text{C}=\text{O})$ stretching vibration peak is observed at 1807 cm⁻¹. In squaric acid, weak peaks at 512 cm⁻¹ and 623 cm⁻¹ are attributed to localised C=O stretching vibrations [29-32]. The broad band around 2300 cm⁻¹ is due to the O-H stretching vibration of squaric acid. The peak frequency values of the C-C and C-O stretching vibrations of squaric acid were observed in the range of 1490-1550 cm⁻¹, centered around 1500 cm⁻¹, with small shifts attributed to hydrogen bonds effects. The peak of the O-H stretching in the DS complex is observed at 3367 cm⁻¹ respectively. Besides, the strong and broad peak of $\nu(\text{C}-\text{C})$ and $\nu(\text{C}-\text{O})$ vibrations, characteristic for squaric acid, is observed at 1497 cm⁻¹ in the complex. These strong and broad bands indicate that the presence of the squarate anion in the complex. The absence of the diffuse band around 2300 cm⁻¹ in the IR spectrum of squaric acid in the complex suggests that the hydrogen in the squaric acid ligand is separated from the structure, referring to the formation of the complex where it is coordinated to the piperidine group of donepezil. In the IR spectrum of squaric acid, the peaks of $\nu(\text{C}=\text{C})$ at 1652 cm⁻¹ and $\nu(\text{C}=\text{O})$ stretching vibrations at 1807 cm⁻¹ were observed at the expected frequencies in the DS complex. The appearance of peaks at 1665 cm⁻¹ in the higher energy region in the DS complex, compared to squaric acid, is attributed to C=C stretching vibrations.

The occurrence of these values in the higher energy region, as compared to the IR spectrum of squaric acid, reveals that DS coordinates through the nitrogen atoms in piperidine. In the IR spectrum of the complex, a robust peak in the range of 1313-1217 cm⁻¹ contributes to the $\nu(\text{C}-\text{N})$ and $\nu(\text{C}=\text{C})$ stretching vibrations of the donepezil

ligand, while the aromatic $\nu(\text{C-H})$ stretching vibrations of this ligand manifest around the 2929 cm^{-1} region. The absence of aromatic or aliphatic C-H groups in the squarate anion makes the peaks in this region indicative of the presence of the donepezil ligand in the structure.

The band at 2702 cm^{-1} corresponds to $\nu(\text{N-H})$, participating in the hydrogen bonds. As the sole proton donor, squaric acid transfers its proton from OH groups to the N atom, leading to the formation of a DS complex (Figure 1).

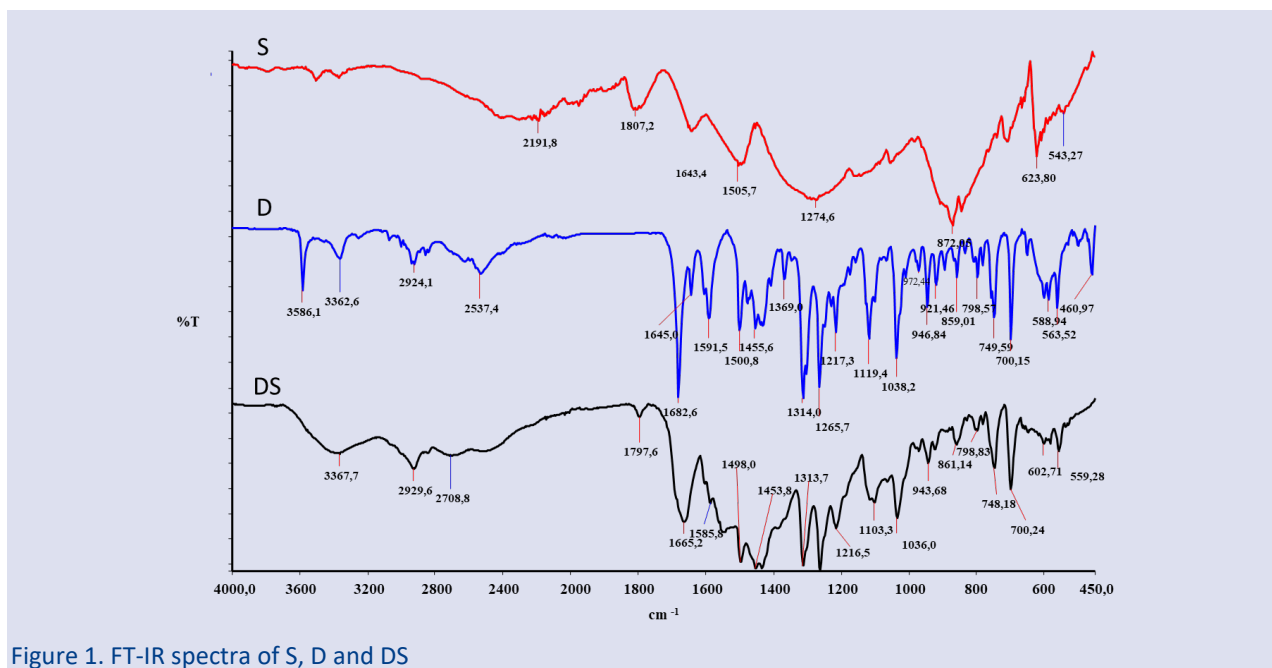


Figure 1. FT-IR spectra of S, D and DS

The aliphatic and aromatic protons in the structure of the DS hybrid compound exhibited peaks in the ^1H NMR spectra, as generally expected. Upon analyzing the hydrogen NMR results of the synthesised compound, where methoxy is at the 5th position of the indanone ring, several noteworthy details emerged. The methoxy protons observed at 3.90 ppm in the starting material did not vary significantly across the electronic environment

due to the distance to altering substituents and peak at 3.87 or 3.79 ppm. The aromatic protons at the 4th, 6th and 7th position of the ring were predominantly observed as doublets, doublets of doublets and doublets, respectively, and in some cases as multiplet intertwined with other protons. Their chemical shift values were 7.05, 7.09, 7.41, 7.50 ppm, respectively (Figure 2).

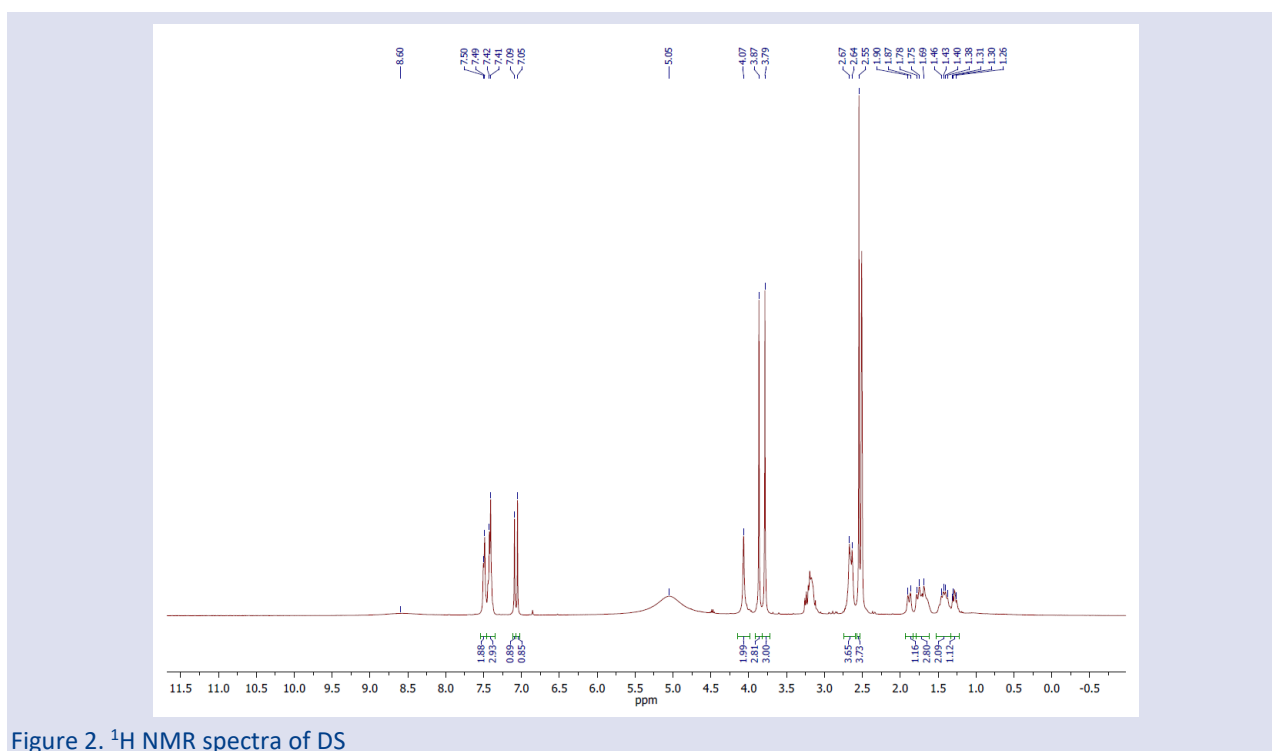


Figure 2. ^1H NMR spectra of DS

The common structural components in the synthesised compound gave peaks in the ^{13}C NMR spectra, aligning with general expectations. The total number of carbons in the spectra of the synthesised compound was determined by considering the identical carbon atoms based on their electronic environment and the expected number of peaks was observed. Specific functional groups (C=O) were observed at 206 ppm in the spectra of the compounds. The remaining aliphatic carbons peaked in

the range of 51.71-28.28 ppm and aromatic carbons in the range of 104.31-155.79 ppm, consistent with findings in the literature. In the chemical structure of the synthesised compound, a disubstituted methoxy group is present at the 5th and 6th positions of the indan-1-one ring system. Carbon atoms belonging to this functional group were identified in the range of 56.39- 55.89 ppm in the spectra (Figure 3).

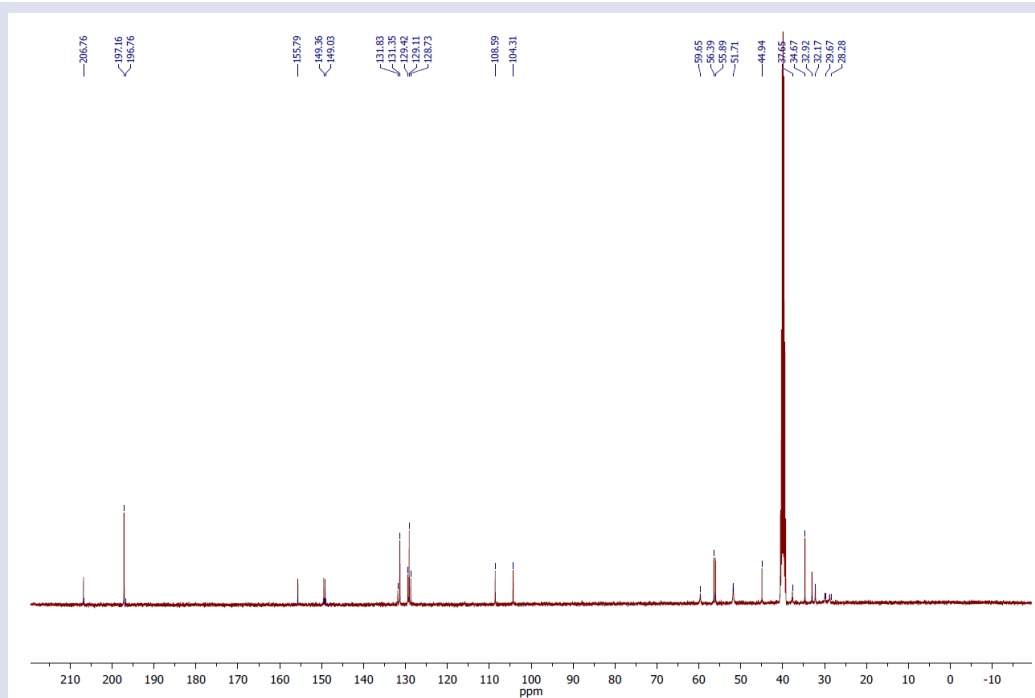


Figure 3. ^{13}C NMR spectra of DS

DNA Binding Studies

UV-Visible Titration Experiments

Many natural or synthetic drugs function as analogs in protein-nucleic acid recognition studies, offering site-specific reagents for molecular biology. Therefore, investigating drug-DNA interaction is crucial for understanding the molecular mechanisms of drug action and designing specific DNA-targeted drugs [33]. Spectroscopic methods play a pivotal role in understanding the drug-DNA binding mechanism and identifying structural deformations in the double helix during complex formation with molecules [34, 35]. Among various spectroscopic techniques, UV-vis spectroscopy stands out as one of the most simple and popular techniques employed to study small molecules-DNA interaction [34]. There are three main modes of non-covalent interactions through which drug molecules bind to DNA.

Possible bonding modes include electrostatic bonding, groove bonding, and intercalative bonding. Intercalators typically demonstrate a hypochromic effect with a significant redshift, while minor-groove binders may show an occasional hyperchromic effect with little or no wavelength shift [35]. The Figure 4-5 displays the absorption spectra of DS and S in the absence and presence of FSds-DNA. DS independently depicts an

absorption maximum at 266 nm in the absence of FSds-DNA, as indicated in the dotted spectra. Significant changes in DS UV-vis bands confirmed the DS-FSds-DNA interaction. DS-FSdsDNA mixed solutions were prepared by adding different concentrations of FSdsDNA to the DS solution. Upon the addition of various concentrations of FSds-DNA solutions to the DS solution, there was a noticeable increase in the intensities of the absorption peaks. While this indicated the expected hyperchromic effect, a blue shift of up to 7 nm was observed at the wavelength of maximum absorption. Generally, the groove binding interaction between small molecules and FSds-DNA results in hyperchromism and hypsochromism in the absorption bands. The addition of FSds-DNA solution to fixed concentrations of DS and S resulted in an increase in absorbance values and a blue shift of the wavelength. Thus, the interaction mode of DS and S binding with FSds-DNA appears to be groove binding. The K_b value of DS was found to be 5.35×10^4 ($\lambda_{\text{max}}=266$ nm) and the K_b value of S was determined to be $4.92 \times 10^4 \text{ M}^{-1}$ ($\lambda_{\text{max}}=271$ nm). When compared to the known intercalator value such as EB ($1.4 \times 10^6 \text{ M}^{-1}$) [24] and reported groove-binding drugs such as gefitinib ($1.29 \times 10^4 \text{ L. mol}^{-1}$) [35], it becomes evident that the K_b values of DS and S align with the groove-binding values. Considering the K_b binding constants, the DNA binding capacity of DS was found to be higher than that of S.

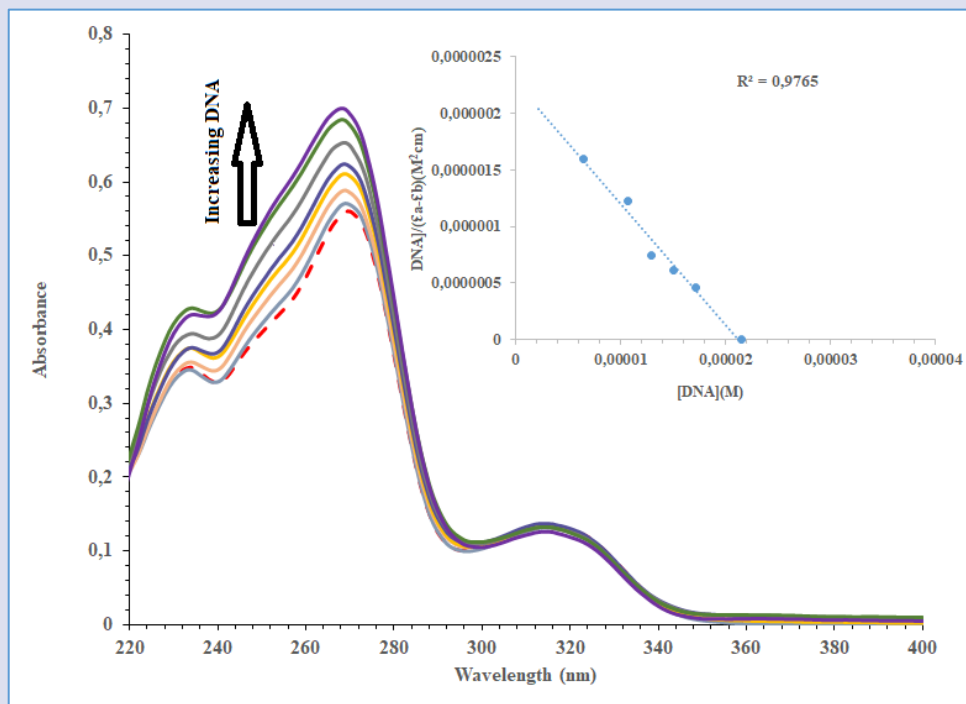


Figure 4. UV-vis absorption spectra of the DS solution resulting from cumulative amounts of FSds-DNA (changes indicated by the arrow). Inset: Graph showing $[DNA]/\epsilon_a - \epsilon_f]$ vs. $[DNA]$

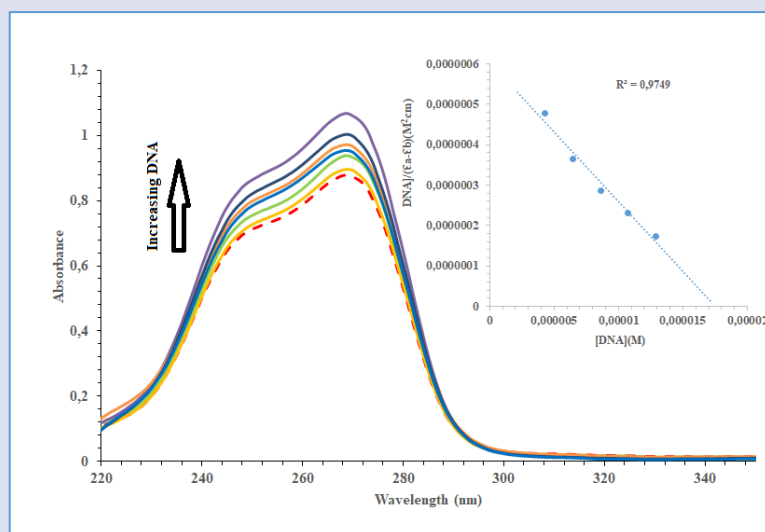


Figure 5. UV-vis absorption spectra of the S solution resulting from cumulative amounts of FSds-DNA (changes indicated by the arrow). Inset: Graph showing $[DNA]/\epsilon_a - \epsilon_f]$ vs. $[DNA]$

Fluorescence Titration Experiments

Fluorescence-based titration experiments were conducted to validate the findings obtained from the UV-vis titration experiment. As is known, the interaction mode of EB on DNA is intercalation [36]. EB is commonly used as a fluorescent probe to verify the binding mode of DNA with small molecules. When inserted between DNA base pairs, EB enhances the fluorescence intensity upon binding to DNA. Compounds with a DNA-like binding mode, such as EB, reduce the EB binding site, thereby quenching the EB-DNA emission intensity. In other words, it reduces the frequency of EB binding to DNA. Upon the addition of the tested compounds to the medium, the intensity of the EB-DNA system in the emission band at 590 nm were noted to decrease with the increasing

concentration of the compound under examination. This effective quenching mode is believed to occur by displacing EB molecules from the EB-DNA system and facilitating the binding of the compound to different regions of the DNA. This study recorded the fluorescence emission spectra of a fixed amount of FSds-DNA and EB in Tris-HCl buffer solution (pH = 7.4), with gradually increasing amounts of DS and S, and the results are summarized in Figure 6-7. The fluorescence intensities of FSds-DNA-EB solutions decreased with the gradual increase in DS and S concentration. The experimental results conclude that there is competitive binding between EB and DS and S on FSds-DNA. Hence, DS and S can bind to regions of FSds-DNA via minor groove binding interaction. K_{sv} values were calculated from the slope of

the Stern-Volmer plot for the quenching of the fluorescence intensity of EB bound to FSds-DNA by DS and S, as shown in Figure 6-7. The K_{sv} quenching constants for DS and S compounds were calculated as $3.5 \times 10^4 \text{ M}^{-1}$ and $1.7 \times 10^4 \text{ M}^{-1}$, respectively. On comparing the calculated values, it becomes apparent that the DS compound exhibits a stronger capability to modify EB-DNA emission.

Moreover, the binding mode of the compounds to the DNA structure involves groove binding rather than intercalation [24]. The decrease in emission intensity is presumed to result from the interaction of DS and S with EB-DNA, changes in the three-dimensional DNA structure or excited-level energy transfer.

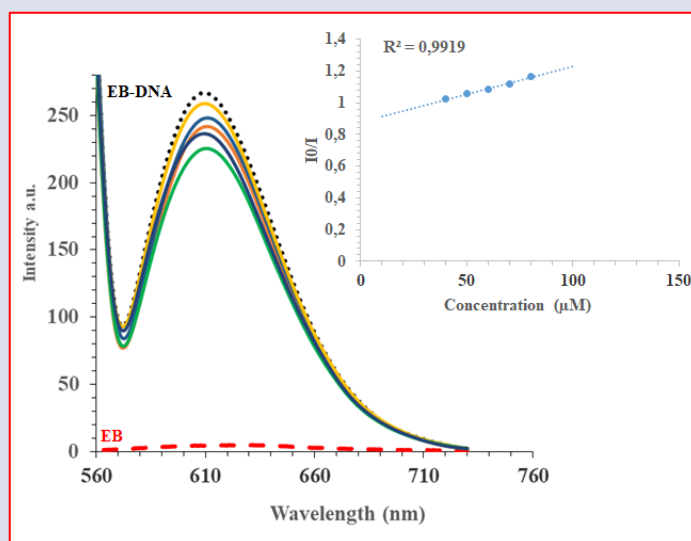


Figure 6. Effect of DS additions at concentrations of 10–100 μM on the emission intensity of the FSds-DNA-bound ethidium bromide in Tris–HCl buffer (pH 7.1); Stern-Volmer graph showing fluorescence titrations of the DS with FSds-DNA.

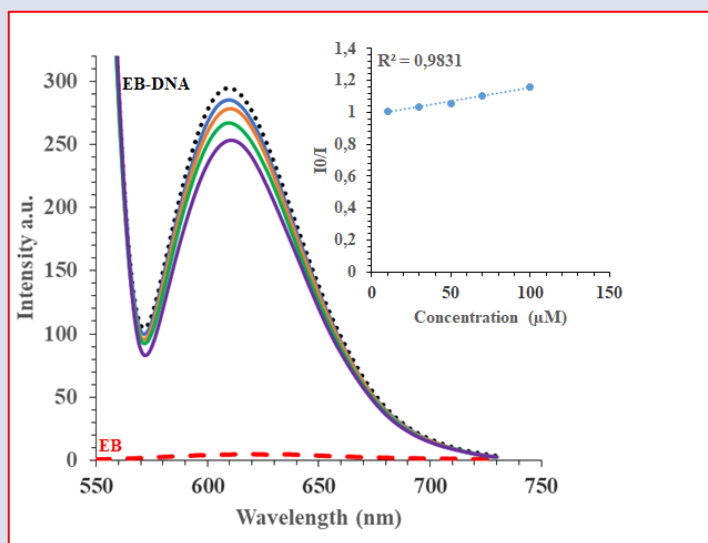


Figure 7. Effect of S additions at concentrations of 10–100 μM on the emission intensity of the FSds-DNA-bound ethidium bromide in 2 mM Tris–HCl buffer (pH 7.1); Stern-Volmer graph showing fluorescence titrations of the S with FSds-DNA

Viscosity Studies

Viscosity measurement is widely acknowledged as an effective and precise method to identify the binding mode between small molecules and DNA [37]. A classical intercalation model proposes that the DNA helix lengthens as base pairs separate to incorporate the compound between the bases, leading to increased DNA viscosity [38]. In contrast, drugs that specifically bind to DNA grooves through partial and/or non-classical intercalation can interact with the DNA strand, reducing its length and generally causing less pronounced or no

change in DNA solution viscosity [38]. The viscosities of FSds-DNA solution ($200 \mu\text{M}$; pH = 7.4) in the absence and presence of DS and S (0 to 60 μM) were measured, and the results are depicted in Figure 8. The results suggested that a very slight change in FSds-DNA viscosity was observed with increasing concentrations of DS and S, and this was not as pronounced as reported for EB, a classical indicator. Therefore, viscosity studies confirm that DS and S bind in the minor groove of FSds-DNA, ruling out the possibility of intercalation [28].

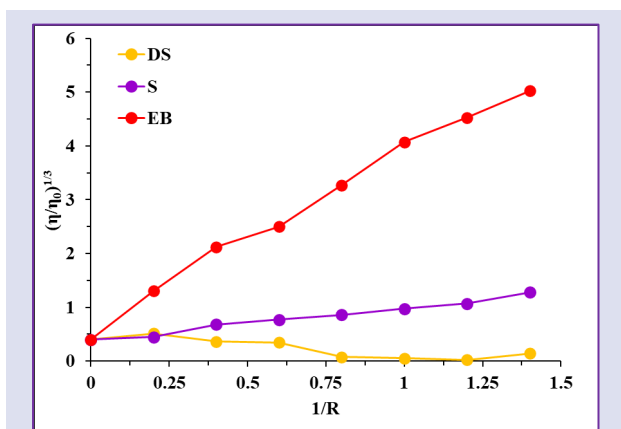


Figure 8. The relative viscosity of FSds-DNA in the presence of different amount of DS and S

Inhibitory Activity Against AChE And BuChE

Cholinesterase enzymes (ChEs) play a role in accelerating the hydrolysis of acetylcholine, a neurotransmitter, thereby reducing acetylcholine levels in the brain. Thus, blocking cholinesterase enhances cholinergic neurotransmission [39]. It utilizes ChE inhibition to alleviate AD symptoms or temporarily slow its progression by restoring cholinergic activity in the brain. The inhibitory activities of DS against AChE and BuChE were assessed using a spectrophotometric method [26], with S serving as the reference compound. For AChE, the IC_{50} value of DS was calculated as 813.7, for S was 1177.8 μM , while for BuChE, DS was 184 and S was 850 μM . The results indicated that DS presented notable inhibitory activity against both AChE and BuChE, with a better selectivity for BuChE compared to S.

Antioxidant Activity

DPPH is characterized as a stable free radical due to the delocalization of the spare electron over the entire molecule, preventing dimerization, a characteristic observed in most other free radicals. The delocalization of electrons imparts a deep violet colour with absorption measured at 517nm. The DPPH radical scavenging activity assay was utilized to determine the total antioxidant activity of the S and DS based on the method described in the literature [27]. This assay was performed for various concentrations (1750 μM , 875 μM , 437 μM , 218 μM and 109 μM) of the S and DS. The Figure 9 signifies the DPPH radical scavenging activity of DS and reference compound (S), expressed as percentage of scavenged DPPH radicals. DS and S showed a decrease in the concentration of DPPH radicals, confirming their scavenging ability. DS exhibited a higher activity in scavenging DPPH radicals compared to S (Table 1).

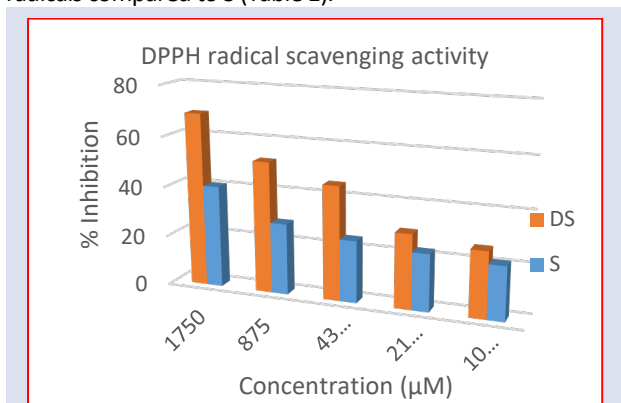


Figure 9. The antioxidant activity of S and DS with DPPH spectrophotometric assay.

Table 1. DPPH antioxidant activities of S and DS.

Sample	DPPH radical scavenging activity assay (IC_{50} value in μM)
S	1055
DS	918

Conclusion

This study synthesized a hybrid molecule by combining donepezil/squaric acid (DS), aiming for its potential application in the treatment of AD. The structure of the DS hybrid molecule was elucidated by FTIR and $^1\text{H}/^{13}\text{C}$ NMR spectroscopy. The binding interactions of DS and S to Fsd-DNA were thoroughly investigated through various experimental methods, including absorption spectrum measurements, fluorescence studies and viscosity measurements. The DNA binding constants for DS and S; K_b were determined using Uv-Visible absorption and fluorescence spectroscopy methods.

The binding of DS with Fsd-DNA resulted in minor hypochromism with no change in the absorbance maximum and fluorescence quenching with minimal shift in the emission maximum, indicative of a groove binding mode of the interaction. Calculated binding constants revealed that DS had a higher interaction with DNA than S. Besides, DS demonstrated higher DPPH scavenging activity in comparison to S. In vitro inhibitory effects of DS and S against AChE and BuChE put forward that DS exhibited stronger inhibitory activity than S.

The preliminary biological activity results reported in our study are promising for obtaining more comprehensive structure-action relationships with derivatizations on the skeletal structure, determination of the type of ChE inhibition by kinetic studies, molecular modeling and toxicity studies and testing of compounds in animal models according to these possible results. In conclusion, the synthesized DS molecule is thought to be a promising scaffold structure in the treatment of neurological diseases. In future studies, we plan to carry out further bioactivity studies on this structure and to obtain broader structure-effect relationships by synthesizing possible molecules with similar skeleton.

Acknowledgments

The author is grateful to the Kahramanmaraş Sutcu Imam University, Scientific Research Projects Unit (KSU-BAP 2019/3-21 M) for the financial support.

Conflict of Interest

There are no conflicts of interest in this work.

References

- [1] Carmo C.M., Mendes E., Jesus P.M., Paula F.A., Marco C.J., The Multifactorial Nature of Alzheimer's Disease for Developing Potential Therapeutics, *Curr. Top. Med. Chem.*, 13 (15) (2013) 1745–1770.
- [2] Mayeux R., Sano M., Treatment of Alzheimer's Disease, *N. Engl. J. Med.*, 341 (22) (1999) 1670–1679.
- [3] George G., Koyiparambath V.P., Sukumaran S., Nair A.S., Pappachan L.K., Al-Sehemi A.G., ... & Mathew B., Structural Modifications on Chalcone Framework for Developing New Class of Cholinesterase Inhibitors, *International Journal of Molecular Sciences*, 23 (6) (2022) 3121.
- [4] Agis-Torres A., Sollhuber M., Fernandez M., Sanchez-Montero J., Multi-Targeted Ligands and Other Therapeutic Strategies in The Search of A Real Solution for Alzheimer's Disease, *Curr. Neuropharmacol.*, 12 (1) (2014) 2–36.
- [5] Svobodova B., Mezeiova E., Hepnarova V., Hrabnova M., Muckova L., Kobrlova T., ... & Korabecny J., Exploring Structure-Activity Relationship in Tacrine-Squaramide Derivatives as Potent Cholinesterase Inhibitors, *Biomolecules*, 9 (8) (2019) 379.
- [6] Chen P.H., Dong G., Cyclobutenones and Benzocyclobutenones: Versatile Synthons in Organic Synthesis, *Chemistry—A European Journal*, 22 (51) (2016) 18290-18315.
- [7] Elliott T.S., Slowey A., Ye Y., Conway S.J., The Use of Phosphate Bioisosteres in Medicinal Chemistry and Chemical Biology, *Med. Chem. Comm.*, 3 (7) (2012) 735-751.
- [8] Henary M., Cyanine and Squaric Acid Metal Sensors, *Sensors and Actuators B: Chemical*, 243 (2017) 1191-1204.
- [9] Tong C., Liu T., Saez T.V., Noteborn W.E.M., Sharp T.H., Hendrix M.M.R.M., Voets I.K., Mummery C.L., Orlova V.V., Kieltyka R.E., Squaramide-Based Supramolecular Materials for Three-Dimensional Cell Culture of Human Induced Pluripotent Stem Cells and Their Derivatives, *Biomacromolecules*, 19 (4) (2018) 1091-1099.
- [10] Qian X., Jin C., Zhang X., Jiang Y., Lin C., Wang L., Squaramide Derivatives and Their Applications in Ion Recognition, *Prog. Chem.*, 26 (10) (2014) 1701.
- [11] Castro I., Calatayud M.L., Sletten J., Julve M., Lloret F., Squarate and Croconate in Designing One-and Two-Dimensional Oxamidato-Bridged Copper (II) Complexes: Synthesis, Crystal Structures and Magnetic Properties of $[\text{Cu}_2(\text{ApoX})(\text{C}_4\text{O}_4)(\text{H}_2\text{O})_2]\text{N} \cdot \text{NaH}_2\text{O}$ and $[\text{Cu}_4(\text{ApoX})_2(\text{C}_5\text{O}_5)_2] \cdot 6\text{H}_2\text{O}$. *Comptes, Rendus l'Académie Des Sci. IIC-Chemistry*, 4 (3) (2001) 235-243.
- [12] Cheuquepán W., Martínez-Olivares J., Rodes A., Orts J.M., Squaric Acid Adsorption and Oxidation at Gold and Platinum Electrodes, *J. Electroanal. Chem.*, 819 (2018) 178-186.
- [13] Chasák J., Šlachtová V., Urban M., Brulíková L. Squaric Acid Analogues in Medicinal Chemistry, *European Journal of Medicinal Chemistry*, 209 (2021) 112872.
- [14] Olmo F., Rotger C., Ramírez-Macías I., Martínez L., Marín C., Carreras L., Urbanova K., Vega M., Chaves-Lemaure G., Sampedro A., Synthesis and Biological Evaluation of N, N'-Squaramides with High in Vivo Efficacy and Low Toxicity: Toward A Low-Cost Drug Against Chagas Disease, *J. Med. Chem.*, 57 (2014) 987-999.
- [15] Cui D., Prashar D., Sejwal P., Luk Y.Y., Water-Driven Ligations Using Cyclic Amino Squarates: A Class of Useful SN1-Like Reactions, *Chem. Commun.*, 47 (4) (2011) 1348-1350.
- [16] Storer R.I., Aciro C., Jones L.H., Squaramides: Physical Properties, Synthesis and Applications, *Chem. Soc. Rev.*, 40 (5) (2011) 2330-2346.
- [17] Korkmaz U., Uçar I., Bulut A., Büyükgüngör O., Three Forms of Squaric Acid with Pyrazine and Pyridine Derivatives: An Experimental and Theoretical Study, *Structural Chemistry*, 22 (2011) 1249-1259.
- [18] Bulut A., Yesilel O.Z., Dege N., Icbudak H., Olmez H., Büyükgüngör O., Dinicotinamidium Squarate, *Acta Crystallographica Section C: Crystal Structure Communications*, 59 (12) (2003) o727-o729.
- [19] Bartoszak-Adamska E., Dega-Szafran Z., Komasa A., Szafran M., Structural and Spectroscopic Properties of Piperidinium-4-Carboxylic Acid Hydrogen Squarate. *Vibrational Spectroscopy*, 81 (2015) 13-21.
- [20] Sang Z., Song Q., Cao Z., Deng Y., Zhang L. Design, Synthesis, and Evaluation of Chalcone-Vitamin E-Donepezil Hybrids as Multi-Target-Directed Ligands for the Treatment of Alzheimer's Disease, *Journal of Enzyme Inhibition and Medicinal Chemistry*, 37 (1) (2022) 69-85.
- [21] Li Q., He S., Chen Y., Feng F., Qu W., Sun H., Donepezil-Based Multi-Functional Cholinesterase Inhibitors for Treatment of Alzheimer's Disease, *Eur. J. Med. Chem.*, 158 (2018) 463–77.
- [22] Unzeta M., Esteban G., Bolea I., Fogel W.A., Ramsay R.R., Youdim M.B., ... & Marco C.J., Multi-Target Directed Donepezil-Like Ligands for Alzheimer's Disease, *Front Neurosci.*, 10 (2016) 205.
- [23] Qiang X., Sang Z., Yuan W., Li Y., Liu Q., Bai P., ... & Deng Y., Design, Synthesis and Evaluation of Genistein-O-Alkylbenzylamines as Potential Multi-Functional Agents for the Treatment of Alzheimer's Disease, *Eur. J. Med. Chem.*, 76 (2014) 314–31.
- [24] Turgut E., Gungor O., Kirpik H., Kose A., Gungor S.A., Kose M., Benzimidazole Ligands with Allyl, Propargyl or Allene Groups, DNA Binding Properties, and Molecular Docking Studies, *Appl. Organometallic Chem.*, 35 (9) (2021) e6323.
- [25] Kose A., Gungor O., Ballı J.N., Erkan S., Synthesis, Characterization, Non-Linear Optical and DNA Binding Properties of A Schiff Base Ligand and Its Cu(II) and Zn(II) Complexes, *Journal of Molecular Structure*, 1268 (2022) 133750.
- [26] Ellman G.L., Courtney K.D., Andres V., Feather-Stone R.M. A New and Rapid Colorimetric Determination of Acetylcholinesterase Activity, *Biochem. Pharmacol.*, 7 (2) (1961) 88-95.
- [27] Liu D., Guo Y., Wu P., Wang Y., Kwaku G.M., Ma H., The Necessity of Walnut Proteolysis Based on Evaluation After in Vitro Simulated Digestion: ACE Inhibition and DPPH Radical-Scavenging Activities, *Food Chemistry*, 311 (2020) 125960.
- [28] Gungor O., Kose M., The Biguanide-Sulfonamide Derivatives: Synthesis, Characterization and Investigation of Anticholinesterase Inhibitory, Antioxidant and DNA/BSA Binding Properties, *Journal of Biomolecular Structure and Dynamics*, 41 (24) (2023) 14952-14567.
- [29] Catro I., Calatayud M.L., Sletten J., Lloret F., Julve M., Syntheses, Crystal Structure and Magnetic Properties of $[\text{Ni}_2(\text{C}_4\text{O}_4)(\text{tren})_2][\text{ClO}_4]_2$ and $[\text{Ni}_2(\text{C}_4\text{O}_4)(\text{tren})_2(\text{H}_2\text{O})_2][\text{ClO}_4]_2$ (tren=tris(2-aminoethyl)amine), *Journal Chemical Society Dalton Translation*, 5 (1997) 811-817.
- [30] Mondal A., Das D., Chaudhuri N.R., Thermal Studies of

- Nickel(II) Squarate Complexes of Triamines in The Solid State, *Journal of Thermal Analysis and Calorimetry*, 55 (1999) 165-172.
- [31] Maji T.K., Das D., Chaudhuri, N.R., Preparation, Characterization, and Solid State Thermal Studies of Cadmium(II) Squarate Complexes of Ethane-1,2-Diamine and Its Derivatives, *Journal of Thermal Analysis and Calorimetry*, 63 (2001) 617-625.
- [32] Das D., Ghosh A., Chaudhuri, N.R., Preparation, Characterization, and Solid State Thermal Studies of Nickel(II) Squarate Complexes of 1,2-Ethanediamine and Its Derivatives, *Bulletion Chemical Society, Japan*, 70 (4) (1997) 789-797.
- [33] Li N., Ma Y., Yang C., Guo L., Yang X., Interaction of Anticancer Drug Mitoxantrone with DNA Analyzed by Electrochemical and Spectroscopic Methods, *Biophysical Chemistry*, 116 (3) (2005) 199-205.
- [34] Chakraborty A., Panda A.K., Ghosh R., Biswas A. DNA Minor Groove Binding of A Well Known Anti-Mycobacterial Drug Dapsone: A Spectroscopic, Viscometric and Molecular Docking Study. *Archives of Biochemistry and Biophysics*, 665 (2019) 107-113.
- [35] Madku S.R., Sahoo B.K., Lavanya K., Reddy R.S., Bodapati A.T.S. DNA Binding Studies of Antifungal Drug Posaconazole Using Spectroscopic and Molecular Docking Methods. *International Journal of Biological Macromolecules*, 225 (2023) 745-756.
- [36] Shi J.H., Liu T.T., Jiang M., Chen J., Wang Q., Characterization of Interaction of Calf Thymus DNA with Gefitinib: Spectroscopic Methods and Molecular Docking, *Journal of Photochemistry and Photobiology B: Biology*, 147 (2015) 47-55.
- [37] Shi J.H., Chen J., Wang J., Zhu Y.Y., Binding Interaction Between Sorafenib and Calf Thymus DNA: Spectroscopic Methodology, Viscosity Measurement and Molecular Docking, *Spectrochimica Acta Part A: Molecular and Biomolecular Spectroscopy*, 136 (2015) 443-450.
- [38] Shahabadi N., Hashempour S. DNA Binding Studies of Antibiotic Drug Cephalixin Using Spectroscopic and Molecular Docking Techniques, *Nucleosides, Nucleotides and Nucleic Acids*, 38 (6) (2019) 428-447.
- [39] Al-ghulikah H.A., Mughal E.U., Elkaeed E.B., Naeem N., Nazir Y., Alzahrani, A.Y.A., ... Shah S.W.A., Discovery of Chalcone Derivatives as Potential A-Glucosidase and Cholinesterase Inhibitors: Effect of hyperglycemia in paving a path to dementia, *Journal of Molecular Structure*, 1275 (2023) 134658.